ISSN 1330-3651 (Print), ISSN1848-6339 (Online)
UDC/UDK 620.172/.173:691.214.8

ANALYSIS ON DEFORMATION CHARACTERISTICS AND ENERGY DISSIPATION OF MARBLE UNDER DIFFERENT UNLOADING RATES

Liming Zhang, Su Gao, Zaiquan Wang, Mingyuan Ren

Original scientific paper

Failure tests were conducted on marble under different unloading confining pressure rates to obtain the energy change curve of whole-process deformation and failure. With increasing unloading rate, the peak stress differences in marble failure were reduced, confining pressure differences in failure increased, the increment ratios of each stress confining pressure were smaller, and the volume deformation was more sensitive to changes in unloading confining pressure. Unloading failure was caused by volume expansion, and the greater the unloading rate was, the easier the rock failure was. With the increasing unloading rate, total absorbed energy increment, elastic energy increment and dissipated energy increment were reduced in the unloading stage of marble. The dissipated energy increment in the unloading process was more than five times that in the loading process, while the elastic energy increment only accounted for 10 % of total stored energy. The unloading process showed increasing dissipated energy, and the geo-stress state of the engineering rock mass determined the level of energy released in failure.

Keywords: *deformation characteristics, energy dissipation, marble, unloading rates*

Analiza značajki deformacije i rasipanja energije mramora pri različitim brzinama rasterećenja

Izvorni znanstveni članak

Ispitivanja oštećenja provodila su se na mramoru kod različitih brzina ograničenja tlaka pri rasterećenju da bi se dobila krivulja promjene energije cijeloga procesa deformacije i oštećenja. S povećanjem brzine rasterećenja, razlike vršnog naprezanja kod oštećenja mramora su se smanjile, razlike ograničenja tlaka su se povećale, omjeri prirasta ograničenja tlaka kod svakog naprezanja su bili manji, a deformacija volumena je bila osjetljivija na promjene ograničenja tlaka kod rasterećenja. Oštećenje kod rasterećenja nastalo je širenjem volumena, i što je veća bila brzina rasterećenja, lakše je dolazilo do oštećenja stijene. S porastom brzine rasterećenja, prirast ukupne apsorbirane energije, prirast elastične energije i prirast disipacije energije smanjili su se u stadiju rasterećenja mramora. Prirast rasipanja energije u postupku rasterećenja bio je pet puta veći od onoga u postupku opterećenja dok je prirast elastične energije pokrivao svega 10 % ukupne akumulirane energije. Postupak rasterećenja pokazao je porast rasipanja energije, a stanje geo-naprezanja stijenske mase odredilo je nivo energije otpuštene u oštećenju.

Ključne riječi: *brzine istovara, mramor, rasipanje energije, značajke deformacije*

1 Introduction

With China's water conservancy and hydropower construction, resource development and the development of rail transport, many rock side slope, underground tunnel and engineering excavation problems have been encountered. In the excavation process, landslides, violent deformation, ground pressure intensification and other phenomena take place frequently, causing huge economic losses and casualties. Therefore, studies on the mechanism of rock mass failure have attracted increasingly widespread attention [1].

Rock engineering excavation is a complex process of loading and unloading, and the deformation characteristics, mechanical parameters and failure mechanisms under unloading stress paths are significantly different from those under loading conditions. Due to the complexity of rock mechanical properties under excavation unloading conditions and diversity of geological predisposing factors, the unloading failure mechanism is very complex and current knowledge is still lacking. Strengthening research on rock failure mechanisms under loading and unloading conditions is of theoretical and engineering significance to deepen our understanding of rock failure mechanisms, as well as to help predict and prevent rock mass disasters.

Currently, only preliminary studies on rock failure mechanisms under unloading stress paths have been carried out. Studies on rock unloading failure characteristics had found that the desired stress increment of unloading failure was smaller than that of loading failure during unloading confining pressure tests of marble in Jinping [2]; the expansion process of marble was significantly affected by the rate of unloading confining pressure[3]; the unloading stress path in the elastic range had no obvious impact on rock strength [4]; and the rock failure surface in the case of unloading failure exhibited tensile failure characteristics [5, 6, 7]. Recent studies on rock failure mechanisms from the perspective of energy change have focused on the release of elastic energy stored in rocks causing rock failure [8, 9], the relationship between energy accumulation, release and destruction in the process of rock deformation [10, 11], the energy evolution laws in rock uniaxial compression testing processes [12, 13], and increasing dissipated energy of rock failure with the increase in loading rate [14, 15].

Unloading rate has significant influences on the mechanical characteristics of rocks. Whether and when actual engineering rock failure occurs is closely related to rock mass stress state and stress drop rates. During underground engineering construction, controlling excavation speed and reducing excavation footage is undertaken to lessen the risk of surrounding rock failure and control the unloading rate. Rock burst and other dynamic disasters induced by excavation unloading under high geo-stress are also closely related to unloading rates. Currently, the influence of unloading rate on rock failure mechanisms is unclear, and research on the influence of unloading rate on energy change during rock failure is still scarce.

2 Experimental scheme

Taking a circular chamber as an example, after underground engineering excavation, the radial stress gradually decreases towards the excavation face as unloading, while tangential stress is generally shown as stress concentration. In the experiment, aiming at the stress path after the excavation of chamber surrounding rocks without timely support, the increase in axial stress was used to simulate tangential stress increase, and confining pressure decrease to simulate radial stress decrease. The precision of the marble specimens met the requirements of the rock mechanics experiment. The experimental test stress path and test data are shown in Figure 1 and Table 1, respectively. The photos of the rock failures are shown in Fig. 2.

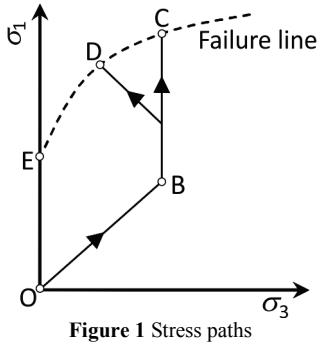

Figure 1 Stress paths

The stress paths of the test are shown in Fig. 1:

(1) Uniaxial compression test (O-E)
(2) Conventional triaxial test (O-B-C)
(3) Unloading test (O-B-D): ① We imposed the confining pressure $\sigma_2 = \sigma_3$ to the desired value; ② With a constant confining pressure σ_3, we increased the axial stress σ_1 to 80 % of the peak strength (we determined 80 % of the peak strength of the rock sample under different confining pressures, based on conventional triaxial test); ③We increased the axial stress σ_1 and reduced the confining pressure σ_3 until the rock sample fractured according to the fixed confining pressure reducing rate of 0,2 ÷ 0,8 MPa/s.

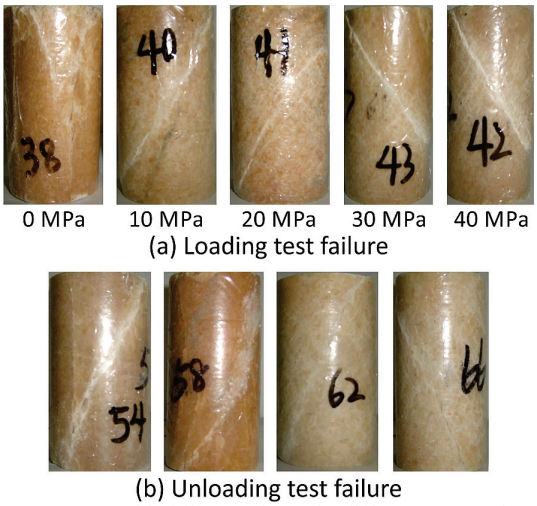

Figure 2 Marble failure modes under different stress paths

3 Analysis on marble unloading failure deformation

3.1 Stress-strain curve

Fig. 3 shows the stress-strain curve of whole-process rock failure under different unloading rates. Before unloading confining pressure, the loading path was exactly the same, so that the four loading process curves almost overlapped, indicating good marble uniformity. In the loading stage, the stress–strain curve showed linear development, with the increased speed of axial strain greater than that of circumferential strain. After unloading the confining pressure, the circumferential strain increased rapidly, while the axial deformation grew slowly, and the volume expanded quickly. The process of the unloading confining pressure is often accompanied by intensive circumferential deformation and volume expansion. Rock unloading failure is caused by intensive expansion along the unloading direction. The unloading rate was increased, and the maximum principal stress of marble undermine was reduced.

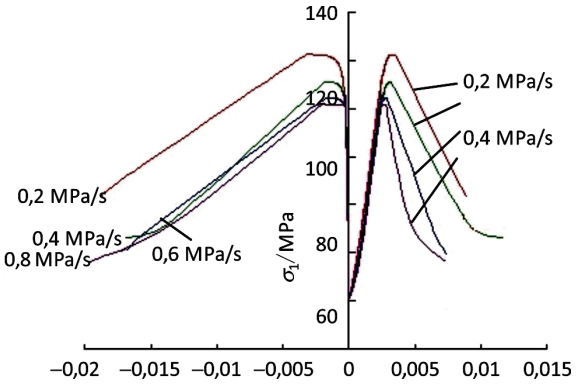

Figure 3 Stress-strain curve of unloading failure

3.2 Stress differences in unloading failure

Fig. 4 shows the change curve of peak stress difference over unloading rate. Under the same confining pressure, the peak stress differences of marble failure were reduced with the increase of the unloading rate. Taking the confining pressure of 20 MPa as an example, with the unloading rates increasing from 0,2 MPa/s, 0,4 MPa/s, 0,6 MPa/s to 0,8 MPa/s, the stress differences in rock failure gradually reduced from 108 MPa, 102 MPa, 98 MPa to 96 MPa respectively, and fast unloading more easily induced rock failure. Reasonable control of construction speed to reduce disturbance on surrounding rocks, and immediately follow-up support is of significance to ensure surrounding rock stability.

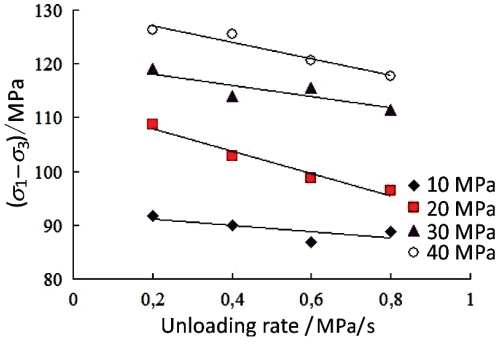

Figure 4 Relationship between stress difference and unloading rate

Table 1 Experimental data of specimens

Initial confining pressure / MPa	Unloading rate / MPa/s	Peak stress σ_1 / MPa	Confining pressure of failure σ_3 / MPa	Peak stress difference $(\sigma_1-\sigma_3)$ / MPa	Confining pressure difference of failure $\Delta\sigma_3$ / MPa	Unloading failure time Δt / s	Total energy of peak / MJ/m^3	Elastic energy of peak / MJ/m^3	Dissipated energy of peak / MJ/m^3	Increment difference of total energy / MJ/m^3	Increment difference of elastic energy / MJ/m^3	Increment difference of dissipated energy / MJ/m^3
10	0,2	98,7	7,0	91,7	2,9	15,0	0,1732	0,1264	0,0468	0,0785	0,0403	0,0382
10	0,4	93,8	3,8	90,0	6,2	15,6	0,1462	0,1166	0,0296	0,0504	0,0289	0,0215
10	0,6	90,2	3,4	86,8	6,6	11,0	0,1221	0,0981	0,0240	0,0284	0,0191	0,0093
10	0,8	90,2	1,4	88,8	8,5	10,8	0,1240	0,0948	0,0291	0,0304	0,0203	0,0101
20	0,2	122,4	13,6	108,8	6,3	31,8	0,2364	0,1713	0,0651	0,1219	0,0630	0,0589
20	0,4	111,0	8,2	102,8	11,8	29,6	0,1979	0,1519	0,0460	0,0734	0,0349	0,0385
20	0,6	104,4	5,6	98,8	14,3	23,8	0,1692	0,1321	0,0372	0,0491	0,0174	0,0317
20	0,8	101,5	5,1	96,4	14,7	18,4	0,1487	0,1213	0,0274	0,0297	0,0097	0,0200
30	0,2	143,3	24,4	118,9	5,6	28,2	0,3208	0,2287	0,0920	0,1476	0,0708	0,0768
30	0,4	134,9	21,0	113,9	9,0	22,6	0,2708	0,1940	0,0768	0,1107	0,0448	0,0659
30	0,6	131,4	15,9	115,5	14,0	23,4	0,2566	0,1892	0,0675	0,0846	0,0335	0,0511
30	0,8	126,3	14,8	111,5	15,1	19,0	0,2432	0,1840	0,0592	0,0543	0,0201	0,0342
40	0,2	160,7	34,4	126,3	5,5	27,8	0,3883	0,2602	0,1281	0,1690	0,0709	0,0981
40	0,4	155,0	29,5	125,5	10,4	26,2	0,3535	0,2598	0,0937	0,1420	0,0540	0,0880
40	0,6	147,9	27,4	120,5	12,6	21,2	0,3182	0,2359	0,0823	0,1044	0,0328	0,0716
40	0,8	143,3	25,7	117,6	14,2	17,8	0,2970	0,2320	0,0650	0,0681	0,0199	0,0482

3.3 Confining pressure differences in unloading failure

Circumferential confining pressure differences from unloading to failure characterizes the influence of changes in confining pressure unloading rate on rock failure, as shown below.

$$\Delta\sigma_3 = (\sigma_3)_0 - (\sigma_3)_1, \tag{1}$$

where $(\sigma_3)_0$ is the confining pressure before unloading, and $(\sigma_3)_1$ is the confining pressure of failure.

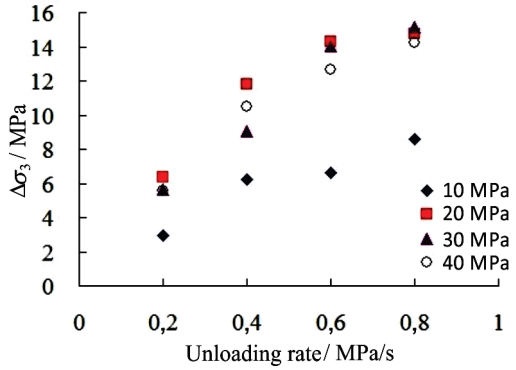

Figure 5 Relationship between confining pressure difference and unloading rate

Fig. 5 shows the relationship between the failure confining pressure differences and unloading rate. When the unloading rate increased, the failure confining pressure differences were gradually enlarged. These results were puzzling as high unloading rate did not easily induce failure. By analyzing the time of failure confining pressure difference, we found that failure time was gradually reduced when the unloading rate was increased, showing that rapid unloading more easily caused rock failure. Taking the confining pressure of 40 MPa as an example, when the unloading rates were increased from 0,2; 0,4; 0,6 and 0,8 MPa/s, the failure confining pressure differences increased from 5,5; 10,4; 12,6 and 14,2 MPa, and the failure times were reduced from 27,7; 26,2; 21,1 and 17,8 s.

3.4 Deformation description of unloading process

To characterize the influence of confining pressure change on deformation, the ratio of the strain increment between the initial point and peak of unloading confining pressure and the reduction of confining pressure was used to analyze deformation, defined as the strain increment ratio of confining pressure. The greater the value, the more sensitive the deformation was to the reduction of confining pressure. The equation is shown below.

$$\Delta\dot{\varepsilon}_i = \frac{\Delta\varepsilon_i}{\Delta\sigma_3}, \tag{2}$$

where $\Delta\varepsilon_i$ (i = 1, 3, V) indicates the axial, circumferential and volumetric strain increment.

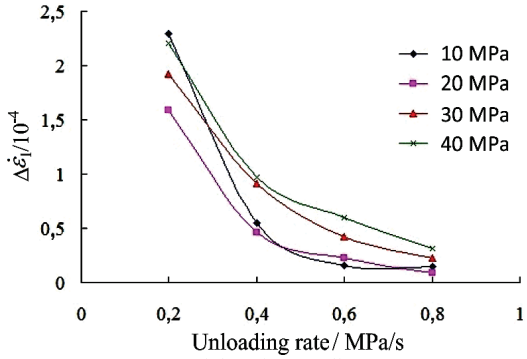

(a) Axial strain compliance

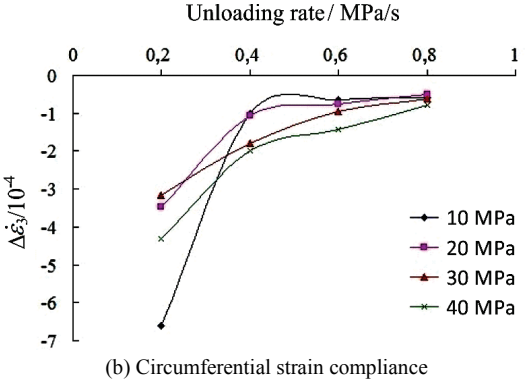

(b) Circumferential strain compliance

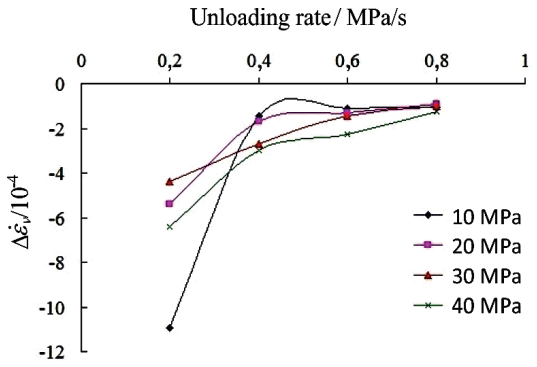

(c) Volumetric strain compliance

Figure 6 Strain increment ratio of confining pressure and unloading rate curves

Fig. 6 shows the relationship between the strain increment ratio of confining pressure and unloading rate. Under the same confining pressure, circumferential and volumetric strain increment ratio of confining pressure $\Delta\dot{\varepsilon}_V$ had a consistent change law with unloading rate of confining pressure. The greater the unloading rate was, the smaller the strain increment ratio of confining pressure $\Delta\dot{\varepsilon}_i$ was. However, the reduction of the lower unloading rate (0,2; 0,4) was larger, and the change of the higher unloading rate (0,4; 0,8) was smaller, indicating that circumferential and volumetric deformation were more sensitive to slow unloading. The axial strain increment ratio of confining pressure was smaller than the circumferential and volumetric increment ratios of confining pressure, indicating that the circumferential and volumetric deformation were more sensitive to the changes in unloading confining pressure, further proving that the unloading failure was caused by volumetric expansion.

4 Energy evolutionary characteristics of marble unloading failure

4.1 Evolutionary process analysis of strain energy

The experimental marble was hard brittle rock. Its strain hardening stage was not obvious, so that it was unable to divide the stage based on the loading deformation process. The loading process had a good correlation to energy conversion. According to the energy change curve of failure process in Fig. 7, the marble failure process was divided into the compaction stage (OA), elastic stage (AB), crack propagation stage (BC) and post-peak failure stage (CD).

In the compaction stage, the absorbed total energy, elastic energy and dissipated energy increased slowly, and most energy was converted into elastic energy for storage, with very little energy consumed. In the elastic stage, dissipated energy increased very little, and absorbed total energy and elastic energy increased with greater load. Total energy and elastic energy curve were substantially parallel to develop, and the external work was mainly stored as elastic energy. In the crack propagation stage, absorbed total energy continued to increase, but elastic energy showed a slow growth rate and reached a maximum at peak strength. The crack propagation stage showed the most obvious characteristics, i.e., rapid increase in dissipated energy. The reduction in confining pressure caused a rapid increase in circumferential deformation, and the quick development and connection of internal microcracks consumed much energy. In the post-peak failure stage, the energy absorbed by rock specimen posterior to Point C was quickly released, and the macroscopic failure surface of the rock specimen was connected.

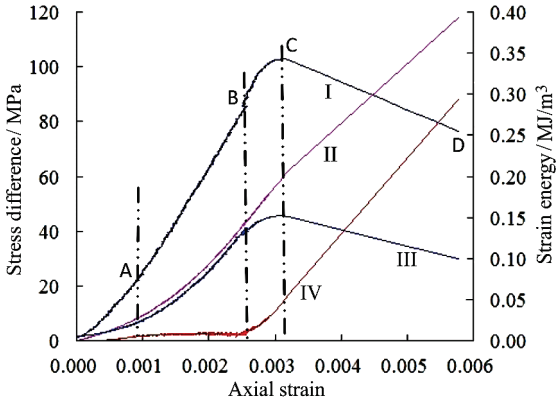

(I - Axial stress, II - Absorbed total energy, III - Elastic energy, IV - dissipated energy)

Figure 7 Energy evolution curve of whole-process unloading failure

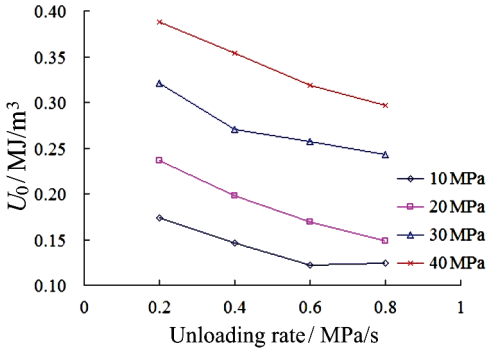

(a) Absorbed total energy

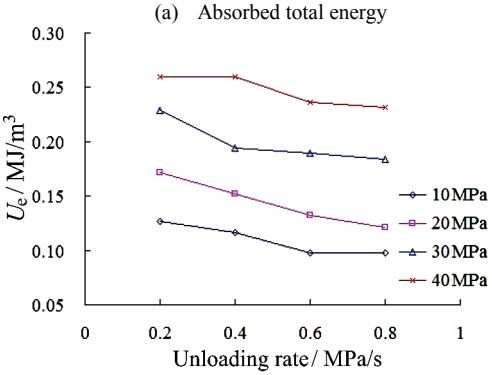

(b) Elastic strain energy

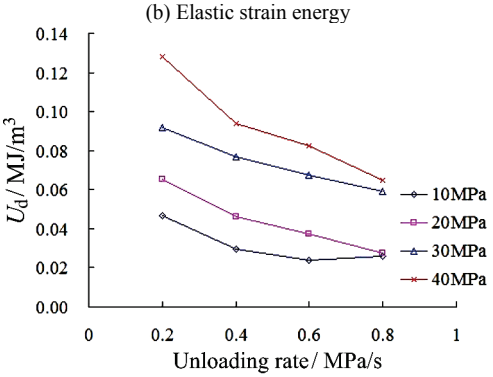

(c) Dissipated strain energy

Figure 8 Relationship between energy and unloading rate at peak strength point

4.2 Energy characteristics at peak strength point

Fig. 8 shows the relationship between strain energy and uploading rate at the peak strength point. The absorbed total energy U_0, elastic energy U_e and dissipated energy U_d of the rock specimen at the peak point were all reduced with increasing unloading rate. The unloading rate influenced the development speed of micro-fractures in the rock specimen. The faster the unloading rate was, the faster the reduction rate of confining pressure and circumferential development and propagation of micro-cracks were, the shorter the formation time of macroscopic failure surface was, and the more abrupt the rock failure was. Taking the confining pressure of 20 MPa as an example, with the unloading rate increasing from 0,2; 0,4; 0,6 and 0,8 MPa/s, the absorbed total energy, elastic energy and dissipated energy of the rock specimen were reduced from 0,24; 0,20; 0,17 and 0,15 MJ/m^3, 0,17; 0,15; 0,13 and 0,12 MJ/m^3, 0,07; 0,05; 0,04 and 0,03 MJ/m^3.

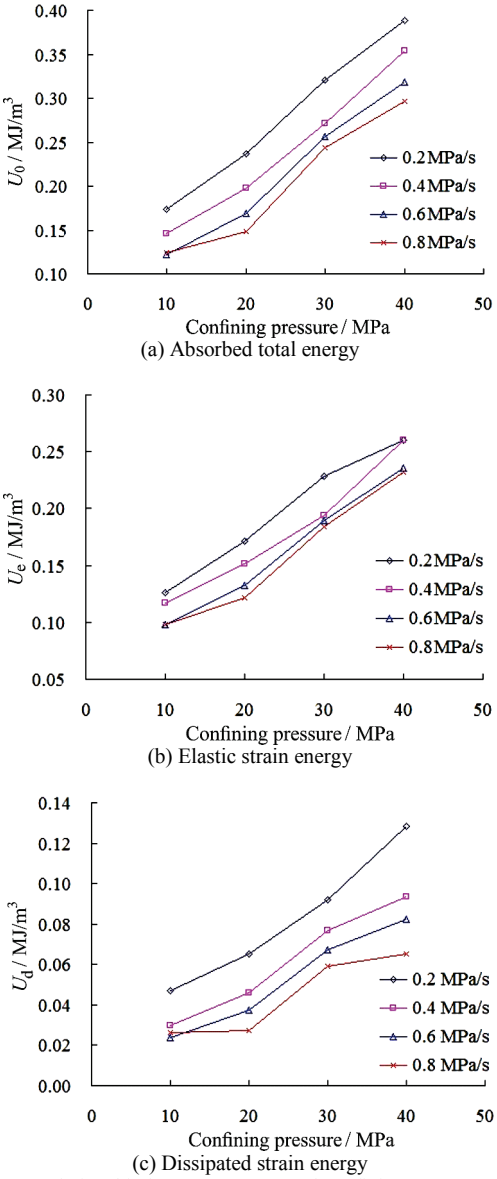

Figure 9 Relationship between energy and confining pressure at peak strength point

Fig. 9 shows the relationship between strain energy and confining pressure at the peak strength point. With increasing confining pressure, the absorbed total energy U_0, elastic energy U_e and dissipated energy U_d of the rock specimen at the peak point all increased. The higher the confining pressure, the slower was the development rate of cracks, the more work the development of internal micro-cracks required to overcome confining pressure, the higher the stored elastic energy, and the greater the dissipated strain energy was, due to crack development and failure surface friction. Taking the unloading rate of 0,4 MPa/s as an example, with the initial unloading confining pressure increasing from 10 to 40 MPa, the absorbed total energy, elastic energy and dissipated energy increased from 0,15; 0,20; 0,27; 0,35 MJ/m^3, 0,12; 0,15; 0,19; 0,26 MJ/m^3 and 0,03; 0,05; 0,08; 0,09 MJ/m^3, respectively.

4.3 Energy increment difference analysis of unloading process

The increment differences in unloading failure energy ΔU represented energy change between the unloading point and peak strength point, reflecting the influence of unloading confining pressure process on the failure energy change, as shown below.

$$\Delta U = U_C - U_B, \tag{3}$$

where U_B is the strain energy at unloading point, and U_C is the strain energy at peak point.

Fig. 10 shows the relationship between energy increment differences and unloading rate. Total energy increment ΔU_0, elastic energy increment ΔU_e and dissipated energy increment ΔU_d all decreased with increased unloading rate. The faster the unloading rate was, the less energy was required to drive rock failure, with failure occurring under smaller energy increments. Taking the confining pressure of 20 MPa as an example, with the unloading rate increasing from 0,2 to 0,8 MPa/s, the increment differences in total energy, elastic energy and dissipated energy were reduced from 0,12; 0,07; 0,05; 0,03 MJ/m^3, 0,06; 0,03; 0,02; 0,01 MJ/m^3 and 0,06; 0,04; 0,03 MJ/m^3, respectively. The increment of elastic energy in the unloading process was smaller, while that of dissipated energy was larger, and the majority of external work was consumed by the internal propagation of rock cracks in the unloading process.

Fig. 11 shows the relationship between energy increment differences and confining pressure. In the unloading process, energy increment was enlarged with increased confining pressure. The higher the confining pressure, the more external work required for failure. Taking the unloading rate of 0,4 MPa/s as an example, with confining pressure increasing from 10 to 40 MPa, the increment differences in total energy, elastic energy and dissipated energy increase from 0,05; 0,07; 0,11; 0,14 MJ/m^3, 0,03; 0,03; 0,04; 0,05 MJ/m^3 and 0,02; 0,04; 0,07, 0,09 MJ/m^3, respectively.

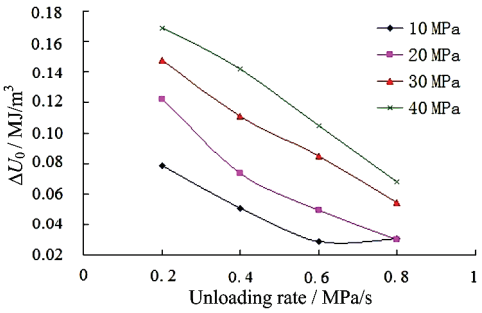

(a) Increment difference of total energy

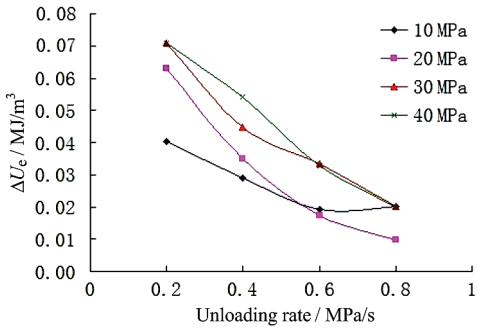

(b) Increment difference of elastic energy

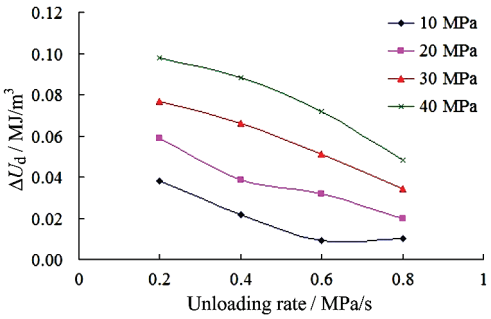

(c) Increment difference of dissipated energy

Figure 10 Relationship between energy increment and unloading rate in the unloading failure process

Fig. 12 shows the energy distribution of typical rock specimens in the loading and unloading stages. The dissipated energy increased substantially in the unloading stage, and was more than five times greater than in the loading process, while absorbed total energy and elastic energy were less than those in the loading process. The driving energy of rock failure (stored elastic energy with release availability) was mainly accumulated in the loading stage prior to the unloading, and the elastic energy that increased in the unloading confining pressure process only accounted for 10 % of total stored elastic energy. Rock failure is a release process of elastic energy stored in the loading stage prior to unloading confining pressure, and the release of elastic energy stored in the loading process is the main reason for unloading failure. The geo-stress state before engineering excavation determines the magnitude of energy released by rocks, and the increment of elastic energy able to be released by the rocks in the excavation stage is very small. Before rock excavation under high geo-stress, a significant amount of released elastic energy is accumulated, which may induce unexpected rock dynamic disasters. Pre-drilling in the front of working faces to release some elastic energy can effectively slow or prevent the failure of surrounding rocks.

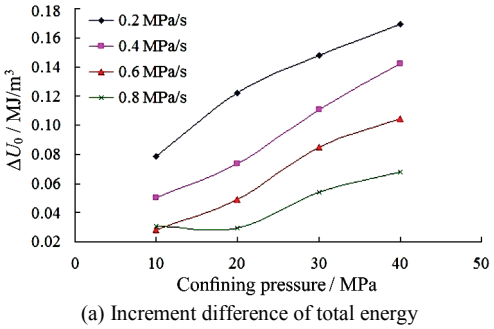

(a) Increment difference of total energy

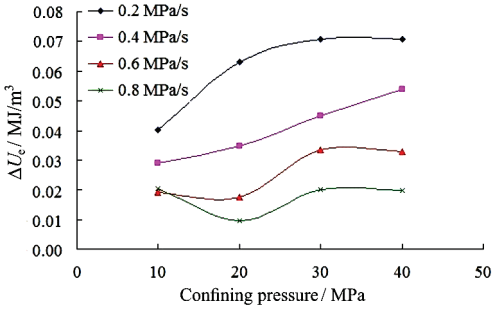

(b) Increment difference of elastic energy

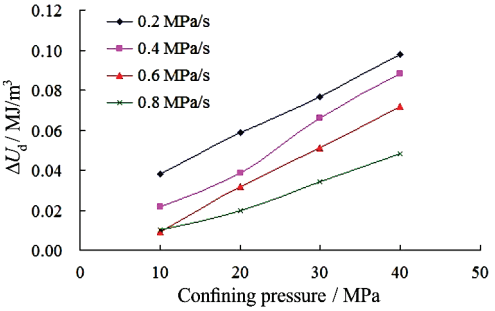

(c) Increment difference of dissipated energy

Figure 11 Relationship between energy increment and confining pressure in the unloading failure process

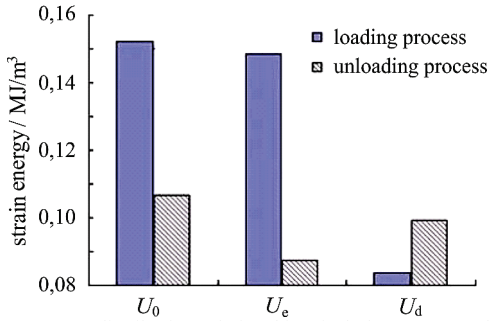

Figure 12 Energy distribution relationship of whole-process rock failure

5 Conclusions

(1) With an increasing unloading rate, the peak stress differences in marble failure decreased, the failure confining pressure differences increased, the strain confining pressure increment ratios were reduced, and circumferential and volumetric deformation became more sensitive to changes in unloading confining pressure. Unloading failure was caused by volume expansion.

(2) In the unloading stage, the increments of absorbed total energy, elastic energy and dissipated energy were all reduced with increasing unloading rate, indicating that the faster the unloading rate was, the

less energy was required to drive rock failure in the loading process.

(3) The loading process was an accumulation process of elastic energy, while the unloading process was an increase process of dissipated energy. The driving energy of rock failure was mainly accumulated in the loading process prior to unloading, and the energy stored in the loading process played a decisive role in unloading failure.

Acknowledgments

This work is supported by the National Natural Science Foundation of China (41472270, 41372298), Qingdao Science and Technology Program (Grant No. 12-1-4-4-(10)-jch), Shandong Province Higher Educational Science and Technology Program (J10LE01) and State Key Laboratory for GeoMechanics and Deep Underground Engineering, China University of Mining & Technology (SKLGDUEK1106).

6 References

[1] Ha, Q. L. Rock slope engineering and unloading nonlinear rock mass mechanics. // Chinese Journal of Rock Mechanics and Engineering. 16, 4(1997), pp. 386-391.

[2] Li, H. Z.; Xia, C. C.; Yan, Z. J.; et al. Study of marble unloading mechanical properties of JingPing hydropower station under high geostress conditions. // Chinese Journal of Rock Mechanics and Engineering. 26, 10(2007), pp. 2104-2109.

[3] Qiu, S. L.; Feng, X. T.; Zhang, C. Q. et al. Experimental research on mechanical properties of deep-buried marble under different unloading rates of confining pressures. // Chinese Journal of Rock Mechanics and Engineering. 29, 9(2010), pp. 1807-1817.

[4] Zhang, K.; Zhou, H.; Pan, P. Z. et al. Characteristics of strength of rocks under different unloading rates. // Rock and Soil Mechanics. 31, 7(2010), pp. 2072-2078.

[5] Yang, S. Q.; Jing, X. W.; Li, Y. S. Experimental investigation on mechanical behaviour of coarse marble under six different loading paths. // Experimental Mechanics. 51, 3(2011), pp. 315-334.

[6] Huang, R. Q.; Huang, D. Experimental research on mechanical properties of granites under unloading condition. // Chinese Journal of Rock Mechanics and Engineering. 27, 11(2008), pp. 2205-2213.

[7] Wu, F. Q.; Tong, L.; Liu, J. Y. et al. Excavation unloading destruction phenomena in rock dam foundations. // Bulletin of Engineering Geology and the Environment, 68, 2(2009), pp. 257-262.

[8] Hua, A. Z.; You, M. Q. Rock failure due to energy release during unloading and application to underground rock burst control. // Tunnelling and Underground Space Technology. 16, 3(2001), pp. 241-246.

[9] Gaziev, E. Rupture energy evaluation for brittle materials. // International Journal of Solids and Structures. 38, 42(2001), pp. 7681-7690.

[10] Xie, H. P.; Ju, Y.; Li, L. Y. Criteria for strength and structural failure of rocks based on energy dissipation and energy release principles. // Chinese Journal of Rock Mechanics and Engineering. 24, 17(2005), pp. 3003-3010.

[11] Zhang, Z. Z.; Gao, F. Experimental research on energy evolution of red sandstone samples under uniaxial compression. // Chinese Journal of Rock Mechanics and Engineering. 31, 5(2012), pp. 953-962.

[12] Zheng, Z. S. Energy transfer process and dynamic analysis during rock deformation. // Science in China (Series B). 34, 1(1991), pp. 104-117.

[13] Huang, D.; Huang, R. Q.; Zhang, Y. X. Experimental investigations on static loading rate effects on mechanical properties and energy mechanism of coarse crystal grain marble under uniaxial compression. // Chinese Journal of Rock Mechanics and Engineering. 31, 2(2012), pp. 245-255.

[14] Zhang, Z. X.; Kou, S. Q.; Jiang, L. G. et a1. Effects of loading rate on rock fracture: fracture characteristics and energy partitioning. // International Journal of Rock Mechanics and Mining Sciences. 37, 5(2000), pp. 745-762.

[15] Stef, Fler. E. D.; Epstein, J. S.; Conley, E. G. Energy partitioning for a crack under remote shear and compression. // International Journal of Fracture. 120, 4(2003), pp. 563-580.

Authors' addresses

Liming Zhang, Associate Professor
College of Science, Qingdao Technological University, Qingdao, Shandong 266033, China
Co-operative Innovation Center of Engineering Construction and Safety in Shandong Peninsula blue economic zone, Qingdao Technological University, Qingdao, Shandong 266033, China
State Key Laboratory for GeoMechanics and Deep Underground Engineering, China University of Mining & Technology, Xuzhou, Jiangsu 221008, China
E-mail: dryad_274@163.com

Su Gao
College of Science, Qingdao Technological University, Qingdao, Shandong 266033, China
E-mail: gaosu1987@qq.com

Zaiquan Wang, Professor
College of Science, Qingdao Technological University, Qingdao, Shandong 266033, China
E-mail: zqwang4521@163.com

Mingyuan Ren
College of Science, Qingdao Technological University, Qingdao, Shandong 266033, China
E-mail: 709151404@qq.com

Location

Situated on the eastern coast of Spain, València was founded in 138BC as a Roman colony. The city, which is the third largest in Spain, has the biggest port on the Mediterranean Sea. A large historic city centre makes València a popular tourist destination with many ancient monuments, museums and sights of interest. València is famous for "Les Falles" – four days and nights of city wide celebrations held each year during March in commemoration of Saint Joseph. Visitors are also drawn to the region for its food with Paella having originated from the city.

Conference Venue

The TRYP València Oceanic Hotel is situated near the centre of València. Only a short distance from the City of Arts and Sciences, the harbour and downtown, the hotel is close to all that the city has to offer. With 200 rooms all with high speed internet access, a 24 hour fitness centre, pool, sauna, bar and restaurant, the hotel has all the amenities guests may require.

Submission Information

Papers are invited on the topics outlined and others falling within the scope of the meeting. Abstracts of no more than 300 words should be submitted as soon as possible.

Abstracts should clearly state the purpose, results and conclusions of the work to be described in the final paper. Final acceptance will be based on the full-length paper, which if accepted for publication must be presented at the conference.

The language of the conference will be English.

Online submission:
wessex.ac.uk/contact2015

Email submission
imoreno@wessex.ac.uk

Submit your abstract with 'Contact and Surface 2015' in the subject line.
Please include your name, full address and conference topic.

Conference Secretariat

Irene Moreno Millan

imoreno@wessex.ac.uk

Wessex Institute
Ashurst Lodge, Ashurst
Southampton, SO40 7AA, UK

Tel: +44 (0) 238 029 3223
Fax: +44 (0) 238 029 2853

For more information visit:
wessex.ac.uk/contact2015

CALL FOR PAPERS

CONTACT AND SURFACE 2015

12th International Conference on Computational Methods and Experiments in Surface and Contact Mechanics including Tribology

21 – 23 April 2015
València, Spain

Organised by
University of Groningen, The Netherlands
University of Bournemouth, UK
Wessex Institute, UK

Sponsored by
WIT Transactions on Engineering Sciences
International Journal of Computational Methods and Experimental Measurements

WESSEX INSTITUTE
ADVANCING INTERNATIONAL KNOWLEDGE TRANSFER

wessex.ac.uk/contact2015

The importance of contact and surface effects in modern engineering and their combined effects has led the organisers to reconvene this 12th International Conference, which covers Computational Methods and Experiments in Surface and Contact Mechanics including Tribology.

The series began in Southampton UK (1993); continued in Ferrara and Milan (1995); Oxford, UK and Madrid (1997); Stuttgart and Assissi (1999); Seville (2001); Crete (2003); Bologna (2005); New Forest (2007); the Algarve (2009); Malta (2011) and Siena (2013).

The papers presented in these conferences are permanently archived in the Wessex Institute eLibrary (http://library.witpress.com), where they are easily accessible to the international scientific community.

Central themes of the conference are surfaces, interfaces and thin films. In general, structural components fail by wear, corrosion and fatigue, that is to say affected and initiated by the surface conditions. Consequently, an appropriate approach is to modify the surface layer of a base material or coat it, so as to provide an enhanced performance. However, in many cases it is the combined effect of wear and corrosion that is damaging and as a result this contributes to an even larger complexity. The complexity of the tribological properties of materials and the economic aspects of friction and wear justify an increasing research effort.

The surface treatment chosen should be suitably related to the problem to be solved. The necessary thickness of the coating depends largely on the applied loading and environmental conditions. This conference will address novel protective layers for advances in sliding wear and low friction.

The range of topics to be discussed regarding Tribology embraces all aspects of concern including reliability, energy applications, advanced materials and corrosion. Tribology problems are essentially interdisciplinary. Engineers and scientists working in this field must be familiar with a wide range of issues, including surface mechanics, material characterization, chemical and biological processes, computer simulation, measurements and many others.

The aim of the conference is to encourage international cooperation amongst scientists and engineers and to exchange new ideas. It deals with fundamental and applied concepts in the interdisciplinary fields of surface and contact engineering, including tribology, in particular focusing on the interplay between applied physics, materials science and computational methods.

Conference Topics

- Surface modification
- Experimental and measurement tests
- Computer simulation
- Surface problems in contact mechanics
- Thick and thin coatings
- Fatigue and fracture mechanics
- Computer methods and components
- Biomedical applications
- Residual stress problems
- Tribomechanics
- Lubrication studies
- Test methods for lubricants
- Wear mechanics
- Tribology in biomechanics
- Case studies

Benefits of Attending

Conference Proceedings Papers presented at Contact and Surface 2015 will be published by WIT Press in Volume 91 of WIT Transactions on Engineering Sciences (ISSN: 1746-4471 Digital ISSN: 1743-3533). WIT Press ensures maximum worldwide dissemination of your research through its own offices in Europe and the USA, and via its extensive international distribution network.

Delegates will have the choice of receiving the conference book as either hard cover or digital format on a USB flash drive. The USB flash drive will, in addition, contain papers from previous conferences in this series.

Indexing and Archiving Papers presented at Wessex Institute conferences are referenced by CrossRef and regularly appear in notable reviews, publications and databases, including referencing and abstracting services such as SCOPUS, Compendex, Thomson Reuters Web of Knowledge and ProQuest. All conference books are archived in the British Library and American Library of Congress.

Digital Archive All conference papers are archived online in the WIT eLibrary (http://library.witpress.com) where they are easily and permanently available to the international scientific community.

Journal Papers After the conference, presenters at Contact and Surface 2015 will be invited to submit an enhanced version of their research for possible publication in the International Journal of Computational Methods and Experimental Measurements published by the Wessex Institute.

Reviews Abstracts and papers are reviewed by members of the International Scientific Advisory Committee and other experts.

Open Access Open Access allows for the full paper to be downloaded from the WIT eLibrary archives, offering maximum dissemination. Authors who choose this option will also receive complimentary access for one year to the entire WIT eLibrary.

Networking Participants can present their research and interact with experts from around the world, becoming part of a unique community.

Reduced Fee for PhD Students The Wessex Institute believes in the importance of encouraging PhD students to present and publish innovative research at their conferences. As a result, the Institute offers PhD students a much reduced conference fee.

Conference Chairmen

J De Hosson
University of Groningen, The Netherlands

M Hadfield
University of Bournemouth, UK

C A Brebbia
Wessex Institute, UK

International Scientific Advisory Committee

M Conte
CSM Instruments, Switzerland

Z Khan
University of Bournemouth, UK

D Northwood
University of Windsor, Canada

V Ocelik
University of Groningen, The Netherlands

Y Pei
University of Groningen, The Netherlands

S Syngellakis
Wessex Institute, UK

Citations When referencing papers presented at this conference please ensure that your citations refer to **Volume 91 of WIT Transactions on Engineering Sciences** as this is the title under which papers appear in the indexing services.